



25th ABCM International Congress of Mechanical Engineering
October 20-25, 2019, Uberlândia, MG, Brazil

COBEM-2019-0906

A SIMPLIFIED MEASUREMENT SYSTEM FOR VIBRATION ANALYSIS ON SMALL LOUDSPEAKER

José Marques B. Sobrinho
Alan Gonçalves Paulo e Silva
Renato Franklin Rangel
Cícero da Rocha Souto

Federal University of Paraíba, Cidade Universitária s/n, 58051-900, João Pessoa, Brazil
josemarquesbasilio@gmail.com
alangps1@gmail.com
renato.rangel@cear.ufpb.br
cicerosouto@cear.ufpb.br

Abstract. *In this work is presented an experimental procedure that can be used to evaluate several vibrational electromechanical devices, such as shakers, loudspeakers, piezoelectric actuators, etc. For the validation an experimental setup was set up to evaluate the responses of a small speaker. This setup is composed of: power supply, amplifier circuit and of conditioning, DAQ 6216, loudspeaker, accelerometer and a person computer with the routine implemented in the software LABVIEW® for the control and monitoring of the system. In the excitation, the Chirp signals were generated to promote a frequency sweep at constant amplitudes of 0.5, 1, 2, 3 and 4 V, resulting in a better analysis of the device. By performing a proper synchronization between the output and input signals in DAQ 6216, it was possible to optimally acquire the signals involved in the system, resulting in the not need to use signal generators and oscilloscopes for analysis of this type. From the presented results it is worth mentioning that the instrumentation developed can be considered of great utility in the characterization of mechanical vibration systems.*

Keywords: *Vibration analysis, Loudspeaker, Instrumentation, Chirp signal.*

1. INTRODUCTION

Data Acquisition Devices (DAQ) are commonly used in conjunction with electronic instrumentation for the process of acquisition and processing of signals, where these represent real-world physical conditions. These phenomena are first collected at electrical magnitude levels and then converted by the ADC of the plate into digital numerical values that can be stored by a computer for further analysis and treatment (Lathi and Green, 2005).

A data acquisition system is generally composed of sensors and transducers (which convert physical parameters into electrical signals), signal conditioning circuits (which process and condition sensor signals in order to filters and amplifiers), analog-to-digital converters (DACs - which convert analog signals into digital values), and communication interfaces with a computer (Oppenheim, 1999).

These graphical interfaces are implemented through microprocessors, hardware and software. A common example is LabVIEW® software and its acquisition boards. LabVIEW® is currently used in marine, aerospace, and research worldwide, both in universities and industry. The advantage of LabVIEW® software and its devices is that in addition to the ease of implementation due to its graphic language through blocks, it allows open manipulation of process variables that is at the discretion of the developer (Hua, 2011).

Since the signals obtained from a physical system are analog and the computers process discrete (binary) signals, it is necessary to apply the sampling theory in the representation of the amplitude and frequency of a given analog signal in a discrete series.

Therefore, for further study of this subject, we sought to implement a sequence of procedures so that it was possible to evaluate signals from a driver-type device. Thus, this work aims to demonstrate that a simplified platform can be used for an adequate analysis in general vibrational devices.

2. EXPERIMENTAL SETUP

In this section we describe the experimental procedures used to analyze the response of the speaker employed in the system.

Figure 1 shows the experimental setup with all the devices used for the proposed study.

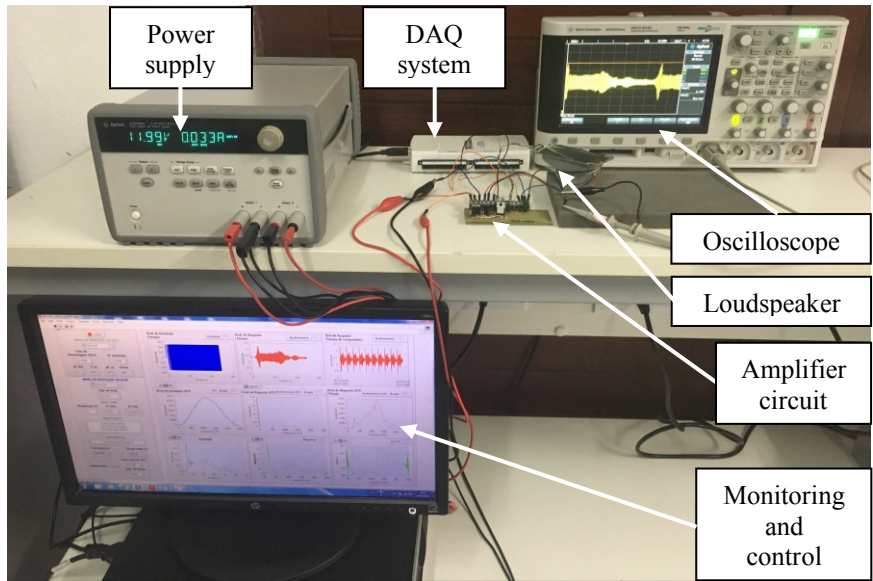


Figure 1. Experimental setup.

The power source is used to supply power to the speaker amplifier circuit as well as to power the accelerometer and the components for its conditioning. Such devices can best be seen in Fig. 2 below.

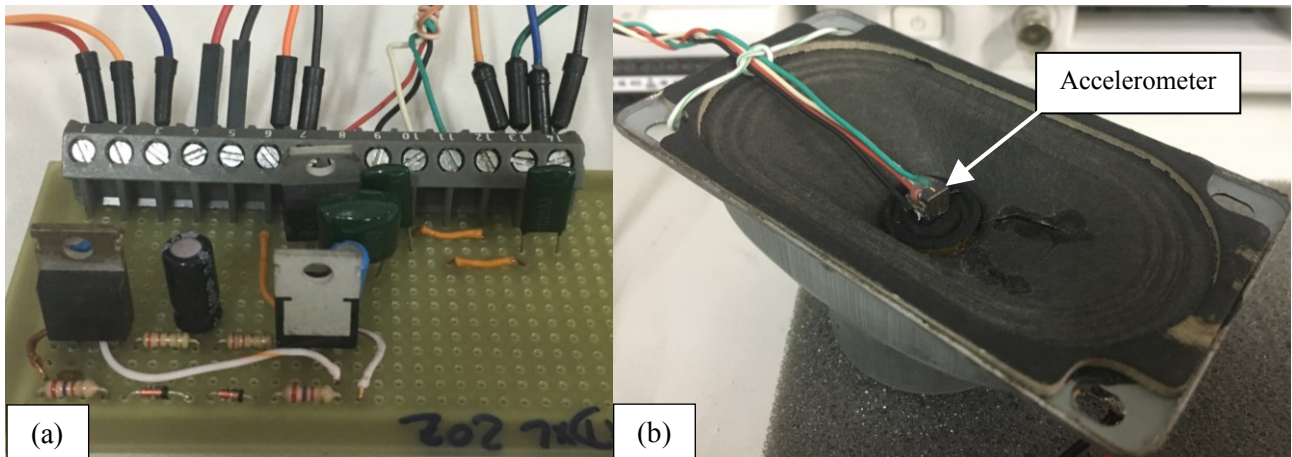


Figure 2. (a) Amplifier circuit, and (b) loudspeaker with accelerometer.

The generation and acquisition of signals were performed by a DAQ 6216 data acquisition device from National Instruments. This device has 16 analog input channels (16-bit, 400 kS / s) and 2 analog output channels (250 kS / s).

The Agilent oscilloscope was used only to verify the accuracy of the signals acquired by the DAQ device 6216. The signals that will be presented later can be correctly acquired with the DAQ device provided that the synchronization between the output and input signals is guaranteed. In addition, the sampling parameters must have direct relations with the type of signal used.

The routine for the control and monitoring of process variables related to the speaker was implemented in LabVIEW® software. The front panel can best be seen in Fig. 3 below, where all variables and graphs analyzed in the system are present. These graphs (results) will be detailed in section 3.

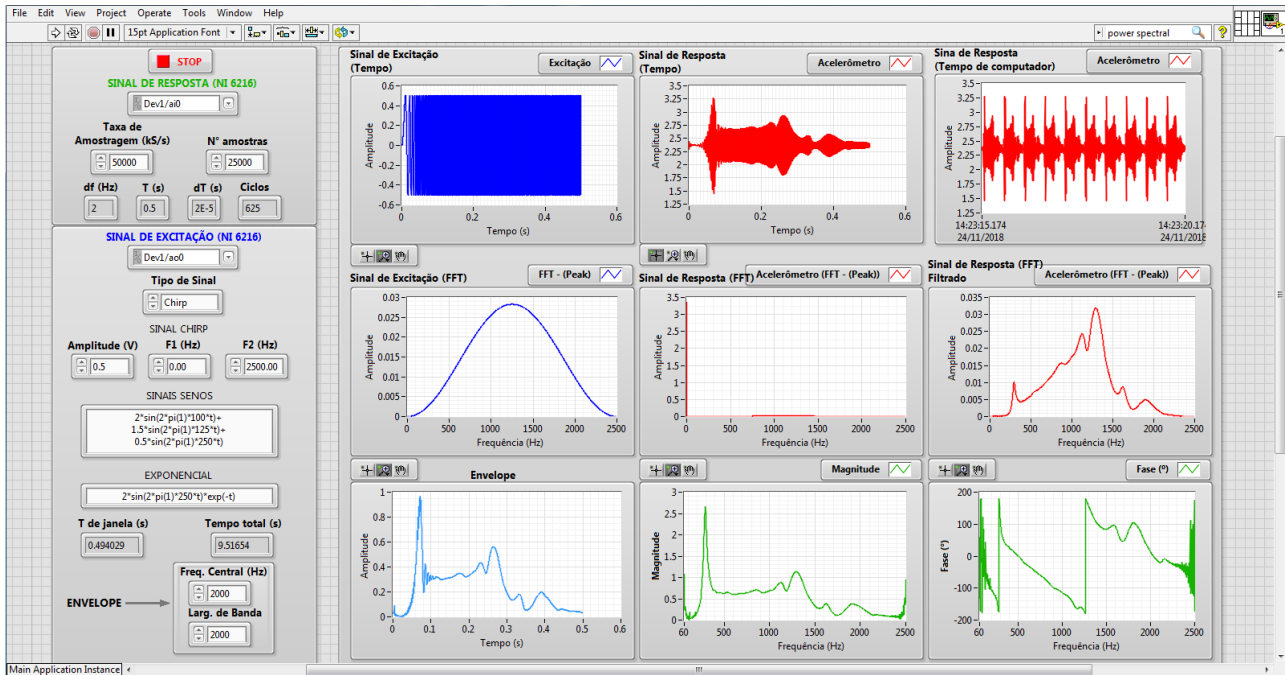


Figure 3. LabView® front panel.

The signal used to analyze the speaker responses was of the Chirp type, as observed in the upper left part of Fig. 3. The Chirp is a dynamic signal that promotes a sweep from an initial low frequency to a high final frequency, or vice versa, keeping the signal amplitude constant. It is a type of signal that is easy to implement and widely used in many measurement systems (Baptista and Filho, 2009; Slepki and Darowicki, 2009; Freitas and Baptista, 2016; Freitas and Baptista, 2017; Taylor et al., 2016; Ribolla et al., 2015; Giulizzi et al. 2015). It can be proved experimentally that the Chirp signal offers better results in comparison to the uniform white noise, Gaussian white noise, periodic random noise, and with that all data presented in this work were obtained with it. The sequence $x[n](n = 0, 1, \dots, N-1)$ of a Chirp signal is given by

$$x[n] = A \cdot \sin\left(\frac{2\pi}{F_S} n \left(\frac{(f_2 - f_1)}{2N} n + f_1\right)\right) \quad (1)$$

In Equation (1), f_1 and f_2 represent the initial and final frequency values, respectively. A is the amplitude, N is the number of samples, and F_S is the sampling rate. The used DAQ device allows the sampling rate of up to 250 kS/s and, as a consequence, a Nyquist frequency of 125 kHz. However, this frequency can easily be increased by choosing other high-speed DAQ devices. The loudspeaker was excited from a level $f_1 = 0$ up to $f_2 = 2500$ Hz using the sampling rate of 50 kHz, which is about 20 times greater than f_2 . The relationship $f_2 N / 2F_S$ provides the total number of cycles and should result in an integer number for the signal only containing integral cycles. The signal containing integral cycles presents little, or no, discontinuity. Thus, there is no spectral leakage, and it is not necessary to window it before computing its DFT. $N = 25000$ and replacing all the other parameters previously defined in (1), the Chirp signal with 625 cycles is obtained, and its duration, which is given by the product $N \cdot dT$ (where $dT = 1 / F_S$), is 500 ms.

From the Chirp signal the frequency behavior of the speaker was studied by means of the fast Fourier transform (FFT) and also by its frequency response (FRF) function. In addition, for the analysis of the modulation of the speaker signal response obtained through the accelerometer, the envelope technique was employed. It is noteworthy that the resulting captured signals were obtained from the average packets of 50 signals, so that possible high frequency noises on the signal could be eliminated.

As we will see later by FFT, the excitation that the speaker can promote is attenuated for frequencies below 60 Hz and above 2250 Hz, which is defined as the best range of the device.

3. EXPERIMENTAL RESULTS

In this section we present the results of the analyzes in the time and frequency domain of the speaker. The responses picked up by the accelerometer indicate the type of excitation that the device can provide to an external system, since the mass (inertia) of the accelerometer used is small. With the use of a data acquisition device (DAQ) it has been proven that there is no need to use a signal generator and an oscilloscope to study these types of problems. The comparisons of these analyzes can be observed by the graphs in the course of this section. In addition, finally, graphs of magnitude and phase of the system response are presented for different levels of excitations and frequencies.

Figure 4 shows the excitation signal supplied to the loudspeaker by the DAQ 6216, in this case captured by Agilent oscilloscope. As already described in the previous section, this signal specifically ranges from 0 to 2500 Hz with a constant peak amplitude of 1V. The power spectral density (PSD) of this signal is considered constant over the entire analyzed frequency range.

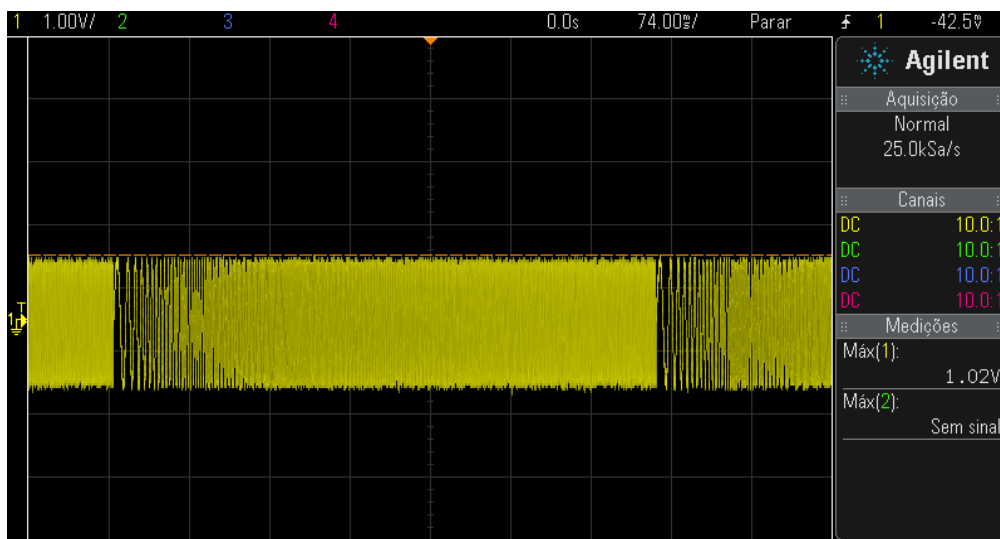


Figure 4. Chirp excitation signal acquired by the oscilloscope.

Figure 5 shows the accelerometer signal, where it is located at the top of the speaker, as already seen in Fig. 2 (b). This signal has a peak amplitude of 0.83 V, since there is an offset level of about 2.54 V. To obtain the acceleration of this sensor a simple mathematical conversion of the value of its sensitivity can be used for this signal .

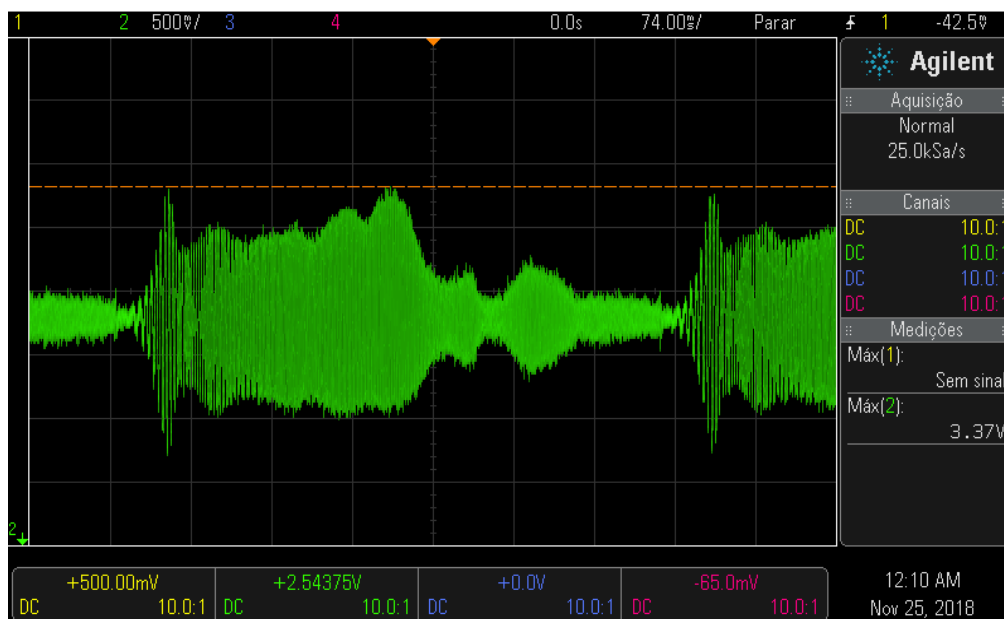


Figure 5. Signal response of the loudspeaker captured by the oscilloscope.

In Figures 6 (a) and (b) the excitation and response signals obtained with the DAQ device 6216, respectively, can be observed. The responses of the device were evaluated for amplitude levels of 0.5, 1, 2, 3 and 4 V peak, in order to perform better analyzes of the system. Comparing the graphs obtained by the oscilloscope and the DAQ 6216 for the voltage of 1V, the complete similarity of these results is clear. This proves the DAQ's ability to capture signals close to its Nyquist frequency.

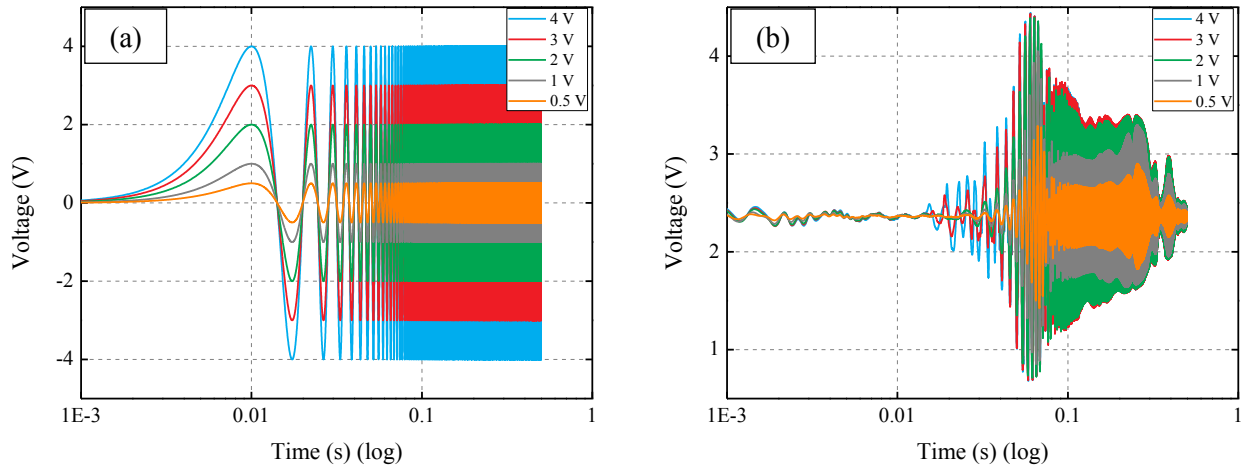


Figure 6. Signals of excitations (a), and responses (b) obtained with DAQ 6216.

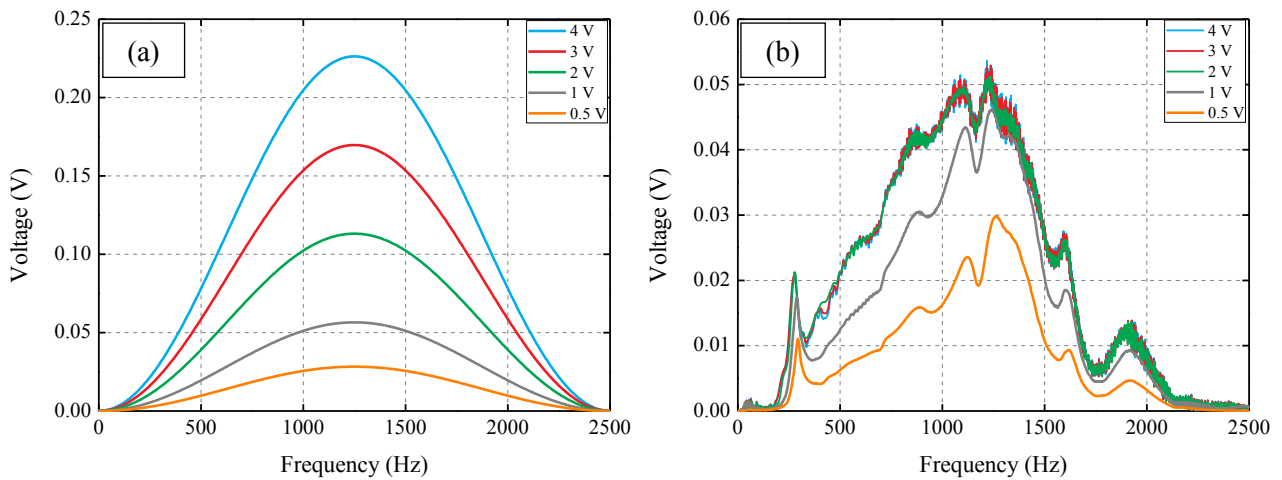


Figure 7. FFT of excitations (a), and responses (b) obtained with DAQ 6216.

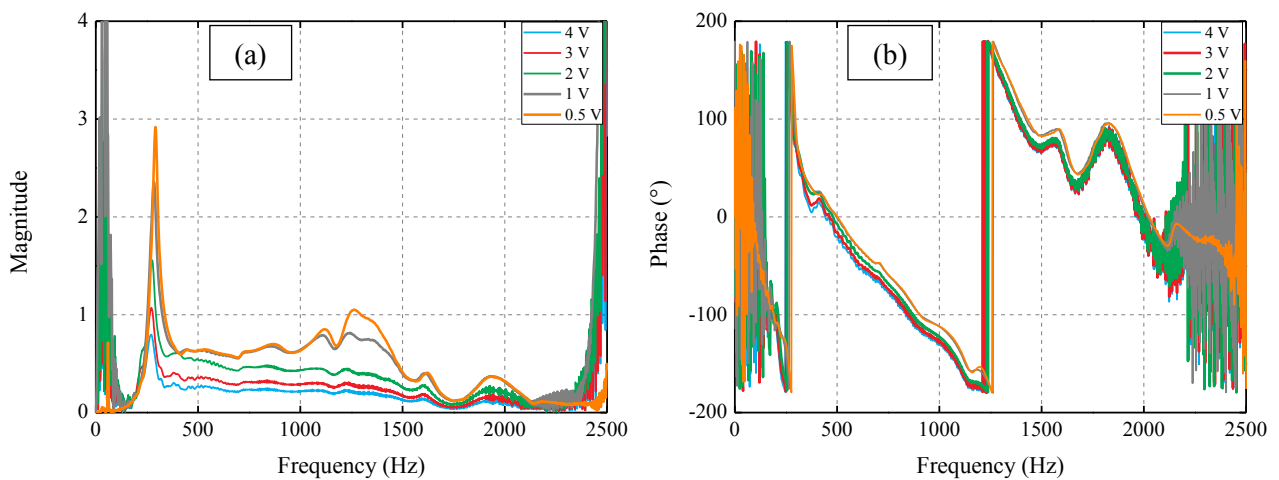


Figure 8. Magnitude (a), and phase (b) of the FRF response signal.

Figures 7 (a) and (b) show the FFTs related to the excitation and response signals of Fig. 6 (a) and (b), respectively. The limits of maximum and minimum amplitude of these signals differ from the values presented in the time domain due to the energy of the Chirp-type signal if it is distributed over the entire frequency range analyzed. These results are used in the calculation of the frequency response function (FRF) of the device, since this function directly relates the response signal to the excitation signal.

Figures 8 (a) and (b) presents the magnitude and phase of the frequency responses (FRF) of the signals picked up by the accelerometer for the different levels of excitation. The side bands of these signals can be discarded, thereby limiting the device's operating range between 60 and 2250 Hz. The system has a maximum transmissibility of approximately 3 around the frequency of 270 Hz. This sudden resonance passage can also be viewed in the graph of the phase of Fig. 8 (b), where the system travels rapidly between -180° and 180° . Other small damped resonances can be observed from 500 Hz.

4. CONCLUSIONS

Based on the analyzes presented in section 3, it is evident that the DAQ device 6216, as well as other devices with similar parameters, can be easily used instead of signal generators and oscilloscopes in signal processing. This clearly implies a great reduction in the cost, the work and the space used for the assembly of the experimental setup.

From the results it is shown that the best range of use of the speaker is between 60 and 2250 Hz. By the response in the magnitude graph, the maximum transmission of energy occurs around the frequency of 270 Hz.

Future analyzes can be used to verify the levels of oscillation of the speaker in terms of displacement as a function of frequency.

5. ACKNOWLEDGEMENTS

The authors thank the Laboratory of Active Systems and Structures and CAPES for the support of equipment and devices used in this study.

6. REFERENCES

- Baptista F. G. and Filho J. V. "A new impedance measurement system for PZT-based structural health monitoring," *IEEE Trans. Instrum. Meas.*, vol. 58, no. 10, pp. 3602–3608, Oct. 2009.
- Diniz, P.S., da Silva, E.A. and Netto, S.L. *Processamento Digital de Sinais-: Projeto e Análise de Sistemas*. Bookman Editora, 2014.
- Freitas, E. S. and Baptista, F. G. "Experimental analysis of the feasibility of low-cost piezoelectric diaphragms in impedance-based SHM applications," *Sens. Actuators A, Phys.*, vol. 238, pp. 220–228, Feb. 2016.
- Freitas, E. S., Baptista F. G., Budoya D. E., and Castro B. A. "Equivalent circuit of piezoelectric diaphragms for impedance-based structural health monitoring applications," *IEEE Sensors J.*, vol. 17, no. 17, pp. 5537–5546, Sep. 2017.
- Giulizzi V., Rizzo P., Milazzo A., and Ribolla E. L. M. "An integrated structural health monitoring system based on electromechanical impedance and guided ultrasonic waves," *J. Civil Struct. Health Monitor.*, vol. 5, no. 3, pp. 337–352, Jul. 2015.
- Hua, Z. "Application of LabVIEW in the design of data acquisition and signal processing system of mechanical vibration," *2011 International Conference on Mechatronic Science, Electric Engineering and Computer (MEC)*, Jilin, 2011, pp. 2551-2554
- Lathi, Bhagwandas Pannalal, and Roger A. Green. *Linear systems and signals*. Vol. 2. New York: Oxford University Press, 2005.
- Oppenheim, Alan V. *Discrete-time signal processing*. Pearson Education India, 1999.
- Ribolla E. L. M., Rizzo P., and Giulizzi V. "On the use of the electromechanical impedance technique for the assessment of dental implant stability: Modeling and experimentation," *J. Intell. Mater. Syst. Struct.*, vol. 26, no. 16, pp. 2266–2280, 2015.
- Slepski P. and Darowicki K. "Optimization of impedance measurements using 'chirp' type perturbation signal," *Measurement*, vol. 42, no. 8, pp. 1220–1225, Oct. 2009.
- Taylor S. G., Raby E. Y., Farinholt K. M., Park G., Todd M. D. "Active-sensing platform for structural health monitoring: Development and deployment," *Struct. Health Monitor.*, vol. 15, no. 4, pp. 413–422, 2016.

7. RESPONSIBILITY NOTICE

The author(s) is (are) the only responsible for the printed material included in this paper.